

Evaluation of Fuji Apple Peel Extract as a Corrosion Inhibitor for Carbon Steel in a Saline Medium

Rosa Vera*, Francisco Figueredo, Andrés Díaz-Gómez, Aurora Molinari

Institute of Chemistry, Faculty of Sciences, Pontificia Universidad Católica de Valparaíso,
Avenida Universidad 330, Placilla (Curauma), Valparaíso, Chile

*E-mail: rosa.vera@pucv.cl

Received: 3 January 2018 / Accepted: 23 February 2018 / Published: 10 April 2018

The present study evaluated the activity of extract obtained from the peel of Fuji apples (*Malus Domestica*) harvested in the region of Valparaiso, Chile, as a potential corrosion inhibitor for carbon steel in a saline medium. The total phenol and flavonoid content in the extract was measured and its main components were identified using HPLC-MS. The inhibition efficiency of the extract was evaluated by mass loss measurements, Tafel polarisation curves and electrochemical impedance spectroscopy, obtaining an inhibition percentage of around 90% at a concentration of 1000 ppm of extract. Adsorption of the extract's components on the surface of the steel followed the Langmuir adsorption isotherm model, implying a physisorption mechanism based on thermodynamic parameters and from the ΔG_{ads}^0 value, which was calculated at -15.16 KJ/mol. SEM was used to verify the presence of an organic layer on the steel, corroborating the adsorption of the organic components from the extract blocking active sites on the steel.

Keywords: carbon steel, Fuji apple, chloride inhibition, adsorption

1. INTRODUCTION

Different types of steel and/or alloys are commonly used in the chemical, petroleum, energy and food production industries, as well as in other areas of daily life. Corrosion is a process that progressively deteriorates metal materials due to interaction with the environmental medium, a process that leads to severe economic and safety problems [1].

Depending on the aggressiveness of the medium, the corrosion process can be controlled by the addition of small concentrations of compounds that act as inhibitors to the electrochemical process [2]. Synthetic/commercial corrosion inhibitors are organic or inorganic compounds that can be highly effective at reducing corrosion, though their use is limited by high operational costs and their damaging effect on the environment. In general, when chemicals such as nitrite, nitrate, chromate and

dichromate are used as inhibitors, they can cause eutrophication of rivers, lakes and seas over time, after being eliminated [3-6].

In recent years, concern for the environment and the sustainability of the planet have led to a renewed search for alternatives that benefit the environment, such as, for example, green corrosion inhibitors obtained from natural extracts [7-9]. At the same time, the processing and manufacturing of food generates by-products and waste products that are rich in bio-compounds that could become a natural source of antioxidant compounds [10]. Extracts from vegetables generally contain compounds with conjugated systems in their structure, as well as nitrogen, oxygen and sulphur atoms [11-12]. These atoms favour the adsorption of such compounds onto metal surfaces, either by the formation of bonds with nonbonding electron pairs of heteroatoms, or by interaction between the metal surface and the π electron cloud of the conjugated system, forming a layer that decreases the corrosion of the metal [13-14].

It is known that apples are a significant source of polyphenolic compounds, including catechins, procyanidins, hydroxyamic acids, chalcones and flavonoids, where the latter are the most abundant and the main component responsible for the antioxidant activity of the fruit [15-16].

In apples, as in other fruits and vegetables in general, the variability of polyphenol profiles is influenced by different factors, such as, farming, mineral nutrition of the plant, seasonality, climate where the plant is grown, level of exposure to the sun, degree of ripeness, storage method, and type of tissue (peel or pulp), among others [16]. It has also been reported that apple processing, to turn it into juice or dehydrate, can lead to a significant drop in phenolic content and in its antioxidant activity [17]. In general, the results show that antioxidant activity of peel extracts are significantly higher (4 to 15 times) than that of the pulp [17-18].

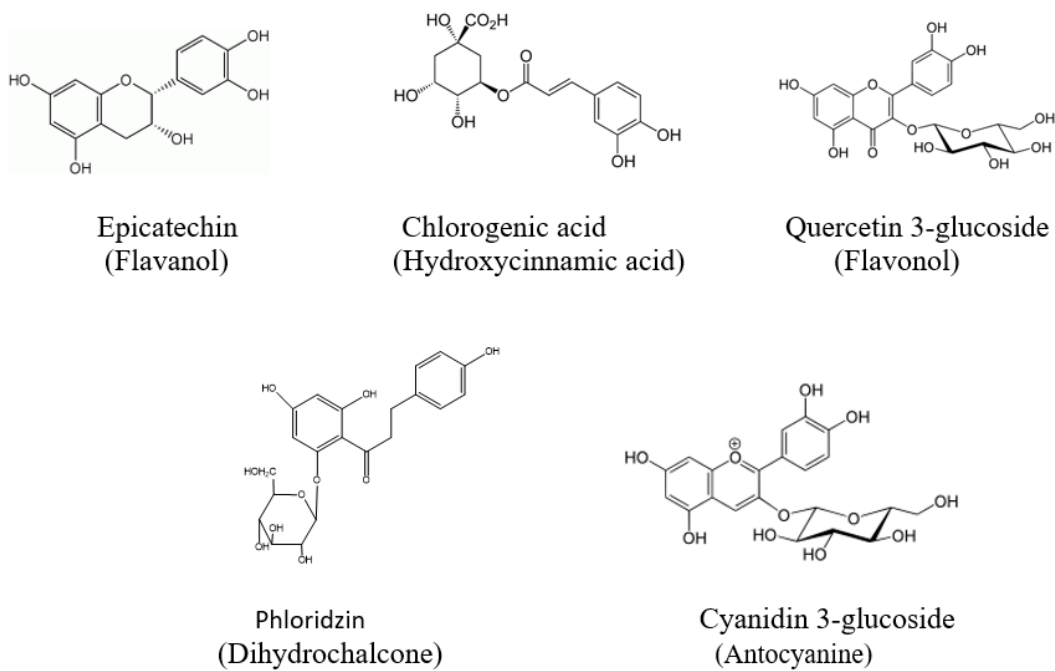


Figure 1. Phenolic compounds isolated from Fuji apple peel extract [19].

Studies have been conducted into the peel of Fuji apples (*Malus Domestica*) harvested in Italy, where its main components were separated and characterised using high-performance liquid chromatography (HPLC) coupled with a diode array detector (DAD) with mass spectrometry (MS). The components found at the highest proportion were quercetin-3-O-glucoside, along with epicatechin, phlorizin, chlorogenic acid and cyanidin-3-O-glucoside (Fig. 1). These, together with other components in the extract, give it significant antioxidant properties mainly attributed to the phenolic compound content (90 mg GAE/100 g dry sample), especially flavonoids [16-20].

In the present study, the results were obtained from evaluating Fuji apple peel extract as a potential corrosion inhibitor for A36 carbon steel in a saline medium (NaCl 0.1 M). The aims of this research is to demonstrate that waste from free fairs that are disposed of as waste can be reused as green inhibitors in the corrosion processes of the materials.

2. MATERIALS AND METHODS

2.1 Materials

The extracts were obtained from Fuji apples acquired at a local market in Valparaiso, Chile, and harvested in the central part of the country during the summer season. They were washed in distilled water, dried with paper tower and stored at -15°C.

The material used for the corrosion tests was A36 steel, the composition of which is shown in Table 1.

Table 1. Composition A36 carbon steel, % in weight.

C	Si	Mn	P	S	Cr	Ni	Mo
0.185	0.136	0.388	0.014	0.008	0.003	0.002	0.002
Al	Cu	Co	Ti	V	W	Sn	Fe
0.037	0.012	0.001	0.001	0.002	0.009	0.001	Rest

2.2 Extract preparation

The peel was separated from the pulp using a ceramic knife. It was then dried in an oven for 48 hours at 60°C. The dry sample was crushed in a stone mortar and tests were then conducted under five sets of extraction conditions: using water at 60°C, 80°C and 100°C, ethanol-water (1:1 v/v) at 60°C, and ethanol-water (1:1 v/v) at 80°C. For extraction, 5 g of dry residue was mixed with each of the aforementioned solvents (1:10 m/v); the mixture was then stirred for 15 minutes, hot filtered and concentrated at low pressure until dry.

2.3 Measurement of Total Phenols (TP)

Total phenol content was measured by UV-Visible spectroscopy applying the colorimeter method of Folin-Ciocalteu [21] and using gallic acid as standard. For the calibration curve, solutions were prepared at concentrations between 4 and 80 mg/L, from a 100 mg/L solution of gallic acid. Of each solution, 100 µl were taken, adding 150 µl deionised water, 125 µl 1N Folin Ciocalteu reagent, and, after a pause of 5 minutes, 625 µl Na₂CO₃ 20% m/v. This was then left to rest for 2 hours at room temperature and in darkness. The absorbance of the samples was measured at $\lambda=760$ nm, using a Perkin Elmer Lambda 3a UV/VIS device.

For the extract analysis, 8 mg of the respective dry residue was dissolved in a 50 mL volumetric flask with deionised water. Of this solution, 100 µL were taken and the procedure described for the calibration curve was then followed. The results were expressed in milligrams of gallic acid equivalent per gram of extract (mg AGA/g extract).

2.4 Measurement of Totals Flavonoids (TF)

The total flavonoid content was measured by UV-Visible spectroscopy by applying the colorimeter method [21], using quercetin as standard. For the calibration curve, solutions were prepared with concentrations between 1 and 25 mg/L from a 100 mg/L quercetin solution. Aliquots of 0.5 ml of each solution were taken, adding 75 µL sodium nitrite at 5%. This was then left to react for 5 minutes, after which 150 µL aluminium trichloride at 10% were added, and after a further 6 minutes, 500 µL 1M NaOH were added. This was left to react for 30 minutes before measurement at $\lambda=490$ nm in a Perkin Elmer Lambda 3a UV/VIS device. For the extract analysis, 8 mg of the respective dry residue were dissolved in 50 ml deionised water, from which an aliquot of 0.5 mL was taken and the procedure described for the calibration curve was then followed. The results are expressed in mg of quercetin equivalent/g extract (mg QE / g extract).

2.5 Infrared (IR) Spectroscopy Analysis

The infrared spectra of the dried and powdered apple peel extract were recorded using a Perkin-Elmer-1600 solid phase spectrophotometer applying the KBr disc method.

2.6 Analysis by Liquid Chromatography – Mass Spectrometry (LC_MS)

The main components present in the apple peel extract were identified and measured using liquid chromatography coupled with reverse phase mass spectroscopy (C18), in negative mode, in tandem, and using an AGILENT 1200s (LC) and AGILENT 6410(MS/MS) with triple quadrupole with electrospray ionisation (ESI). This was done using a GL Sciences Inc. Intersil ODS 4 3.0x50mm (3µm) Column, and binary programme with a gradient of 1% HCOOH (A) and acetonitrile (B) [22].

2.7 Corrosion mass loss tests

The mass loss tests were carried out ASTM G31-72 [23], using test probes of A36 carbon steel measuring 3.0 x 3.0 x 0.2 cm. The metal surface was polished with silicon carbide paper up to 800G, then washed with distilled water and degreased with acetone. The samples were submerged for 24 and 120 hours in a 0.1M NaCl solution in the presence and absence of the extract, at room temperature (25°C). Different extract concentration levels were evaluated: 100, 250, 500 and 1000 ppm. The different extract solutions were prepared by dissolving the necessary amount of extract in the NaCl solution with stirring. After the immersion time, the probes were stripped in accordance with ASTM G1-03 [24]. Corrosion inhibition efficiency was calculated using equation 1. Each test was performed in triplicate.

$$\eta\% = \frac{(W_o - W)}{W_o} \times 100 \quad (\text{equ. 1})$$

where:

W_o : Mass loss in the absence of the extract, (g/cm²)

W : Mass loss in the presence of the extract, (g/cm²)

Once the 120-hour mass loss tests were completed, both in the presence and absence of the extract, the steel surface was examined under a Hitachi SU3500 scanning electron microscope coupled with a Bruker XFlash 410M EDS detector.

2.8 Electrochemical tests

Potentiodynamic polarisation curves were generated using an Autolab PGSTAT302N Potentiostat/Galvanostat. A three-electrode cell was used, containing a platinum counter-electrode, a saturated calomel electrode (SCE) as the reference electrode and the carbon steel as the working electrode. The steel was polished with silicon carbide paper up to 800G, washed with distilled water and degreased with acetone. It was covered with epoxy resin, leaving an exposed area of 1 cm².

The polarisation curves were generated in 0.1M NaCl, varying the extract concentration (0, 250, 500 and 1000 mg L⁻¹), at a scanning rate of 0.2 mV s⁻¹. Before each polarisation, the open circuit potential was stabilised for 30 minutes. The corrosion current density for each system was measured with Tafel gradients. The data obtained were used to calculate inhibition efficiency in accordance with equation 2:

$$\eta\% = \frac{I_o - I}{I_o} \times 100 \quad (\text{equ. 2})$$

where:

I_o : Corrosion current density in the absence of the extract, (A cm⁻²)

I : Corrosion current density in the presence of the extract, (A cm⁻²)

The electrochemical impedance spectroscopy (EIS) measurements were taken in an Autolab PGSTAT302N Potentiostat/Galvanostat using a three-electrode cell (platinum electrode, saturated calomel electrode (SCE) and carbon steel as the working electrode). The same treatment as for the polarisation curves was performed and the test probes were prepared in the same way, leaving an exposed area of 1 cm². The measurements were taken at alternating current signals of 5 mV, in a

frequency range of 100 kHz to 10 mHz, and the open circuit potential was allowed to stabilise for 30 minutes beforehand. The curves were generated in 0.1M NaCl, varying the extract concentration (0, 250, 500 and 1000 ppm).

The results are presented as a Nyquist plot, in which the resistance to charge transfer (R_{ct}) was calculated as the difference in impedance at low and high frequencies, both in the presence and absence of the extract [25].

The inhibition efficiency was calculated using equation 4:

$$E(\%) = \frac{R_{ct,o} - R_{ct}}{R_{ct,o}} \times 100 \quad (\text{equ. 4})$$

where:

$R_{ct,o}$: Resistance to charger transfer in the absence of the extract, ($\Omega \text{ cm}^2$).

R_{ct} : Resistance to charger transfer in the presence of the extract, ($\Omega \text{ cm}^2$).

3. RESULTS AND DISCUSSION

3.1 Extraction

Table 2 shows the extraction yield obtained using different conditions, expressed as a % extraction.

Table 2. Effect of the solvent on the extraction of Fuji Apple Peel.

Solvent	Polarity Index ^a	Extraction yield (%)
Water 100°C	10.2	15.52
Water 80°C	10.2	21.65
Water 60°C	10.2	26.17
Ethanol:Water (1:1) 80°C	7.7	44.81
Ethanol:Water (1:1) 60°C	7.7	61.04

^apolarity index of the solvent [26]. The solvent mixture indices were calculated using the equation $(I_A/100 \times P_A) + (I_B/100 \times P_B)$ where I_A and I_B are the polarity indices of solvents A and B. P_A and P_B are the percentages of solvents A and B in the solvents mixtures.

The highest extract yield was obtained when using the mixture of solvents ethanol:water (1:1 v/v), at a temperature of 60°C, which can be attributed to the polar nature of the phenolic compounds. It can be inferred that an increase in extraction temperature would not lead to an increase in extraction yield, which is likely due to decomposition of the phenolic compounds as a result of the increased time and temperature to which the plant material is subjected during the process, as was shown by Vasconcelos et. al [26]. These researchers performed two types of extraction for coffee residues,

decoction and infusion, both at 100°C, obtaining around 20% more phenolic content for infusion than for decoction.

3.2 Characterisation of the extract

Total phenol and flavonol content

In order to characterise the phenolic compounds present in the Fuji apples harvested in the region of Valparaiso, Chile, the extract obtained from treating dehydrated peel mixed with ethanol:water (1:1) at 60°C was chosen, as these conditions gave the highest extraction yield.

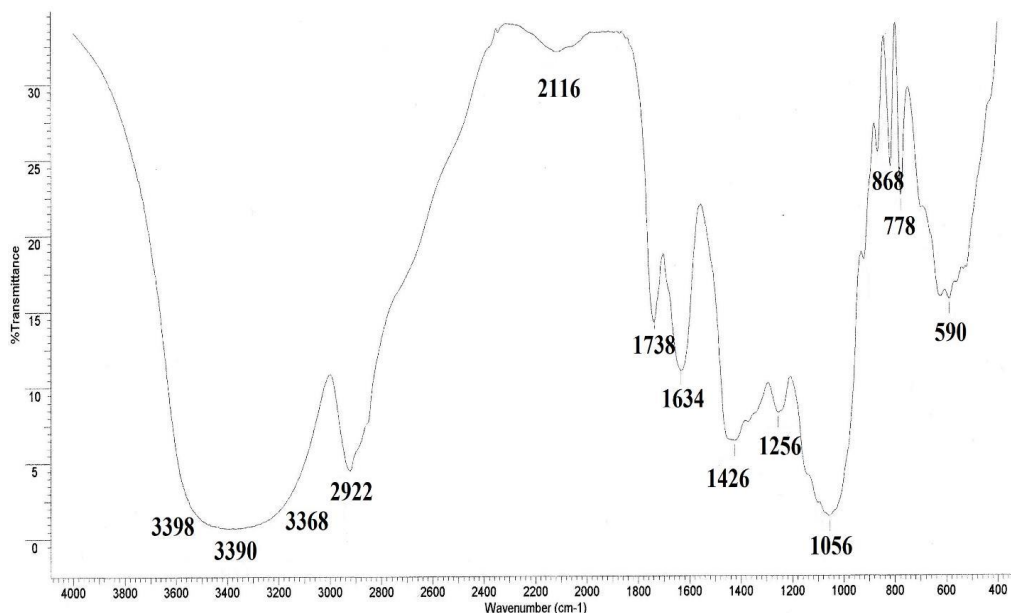
One of the main characteristics of phenolic and flavonolic compounds is that they absorb intensely in the ultraviolet region and in the visible spectrum due to the presence of conjugated aromatic systems [27-28]. The results obtained when measuring total phenol (TP) content and total flavonol (TF) content are shown in Table 3. The lower amount found for flavonol content is because these are a subgroup of phenolic compounds. It should be noted that due to the large number of variables that influence the profile and content of polyphenols present in apples [16-17], in addition to the extraction and storage conditions of the extracts, it is difficult to compare different results from previous studies in the literature [29].

Table 3. Total phenol (TP) and total flavonol (TF) content in the Fuji Apple Peel.

Extract	Total phenol content (mg GAE eq/g extract)	Total flavonol content (mg QE eq/g extract)
Ethanol:Water (1:1) 60°C	132.44 ± 0.09	99.15 ± 0.26

Analysing the apple peel extract using infrared electroscope (FT-IR), the IR spectrum shown in Fig. 2 was found, in which strong absorption around 3600-3200 cm⁻¹ can be seen, associated with the O-H stretching band, and at 2922 cm⁻¹, associated with the C-H stretching. The peaks at 1738 cm⁻¹ and 1634 cm⁻¹ are stretching bands belonging to the carbonyl group (C=O) and C=C bonds, respectively. The peaks at 1426 cm⁻¹ are the stretching bands of the C-C bond and the absorption at 1056 cm⁻¹ is associated with the C-O stretching. The bands denote the main functional groups present, corroborating the presence of flavonoids and phenolic compounds in general in the extract.

The constituent parts with a percentage above 1% in the apple peel extract obtained with ethanol:water (1:1) at 60 °C were identified using Liquid Chromatography with reverse phase Mass Spectroscopy analysis; the results are shown in Table 4. The structures of the two major flavonoids and the quercetin glycosides are shown in Fig. 3.

**Figure 2.** IR spectrum of Fuji Apple Peel extract.**Table 4.** Main constituent parts of the Fuji Apple Peel extract found using HPLC-MS.

Retention Time	Abundance (%)	Base peak	Compound
0.05	1.05	215	Caffeic Acid
0.78	38.49	377	5-Methoxy-6'',6''-dimethyl-3',4'-methylenedioxypyrano(2'',3'',7,8)flavone (Flavone 1)
1.12	44.33	683	3,5,2'-Trihydroxy-7,8,4'-trimethoxyflavone 5-glucosyl-(1->2)-galactoside (Flavone 2)
1.36	2.14	719	7,4'-Dihydroxy-3,5,6,8-tetramethoxyflavone 4'-glucosyl-(1->3)-galactoside
1.57	1.52	439	3,5,8-Trimethoxy-3',4'-methylenedioxy-7-prenyloxyflavone
1.94	1.24	353	Chlorogenic acid
4.43	3.27	463	Quercetin-5-glucoside
5.32	3.15	433	Quercetin-3- \square -L-arabinopyranoside

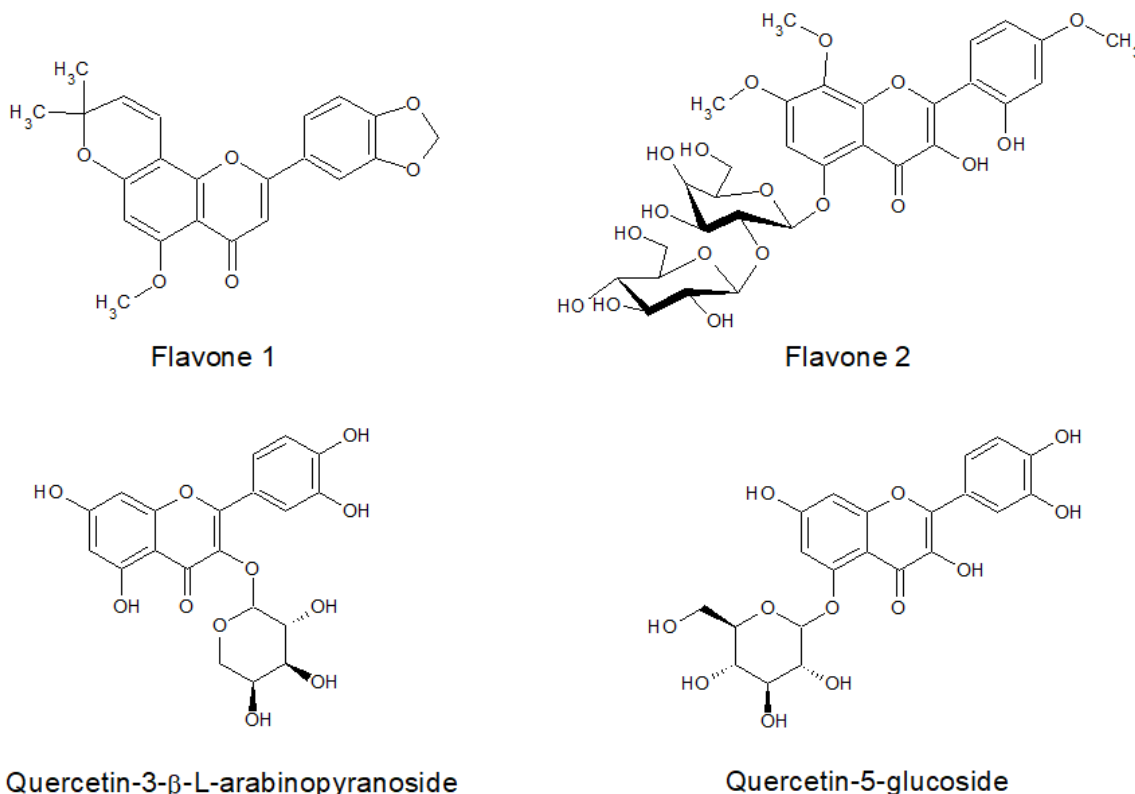


Figure 3. Main flavonoids present in the Fuji Apple Peel extract.

In addition to the compounds mentioned in Table 4, the presence of cyanidin-3-galactoside, cyanidin-3-(6''-dioxalylglucoside), caffeic acid, rutin, isoquercetin, luteolin-5-glucuronide-6''-methyl ester, kaempferol 3-p-coumarate, isochlorogenic acid and neochlorogenic acid was also found, though all at low concentrations (abundance of 0.15 – 0.63 %). Most of the flavonoids and phenolic compounds identified in the extract coincide with the polyphenolic compounds in apples reported in prior studies. However, they differ significantly in the proportions in which they are found. This may be attributed to a series of variables related to the origin of the fruit used (geographic region, seasonality, etc.), as well as the extraction process (solvent, temperature, extraction time, etc.), which significantly influence the composition and the proportions of the phenolic content in the extracts [30].

The corrosion inhibition capacity of the apple peel extract is attributed to the presence of aromatic systems, and to conjugated hydroxyphenol and ketone groups present in the flavonoids. These systems can participate through possible physisorption and/or chemisorption mechanisms that involve interactions between the metal surface and the pairs of nonbonding electrons in the heteroatoms (Fig. 4a) and the $\pi\pi$ -electrons of the conjugated system, as well as the excellent chelation properties of transitory metal ions in iron and other transition metals seen in flavonoids (Fig. 4b). This would lead to the formation of iron complexes on the metal surface that would act as a protective barrier.

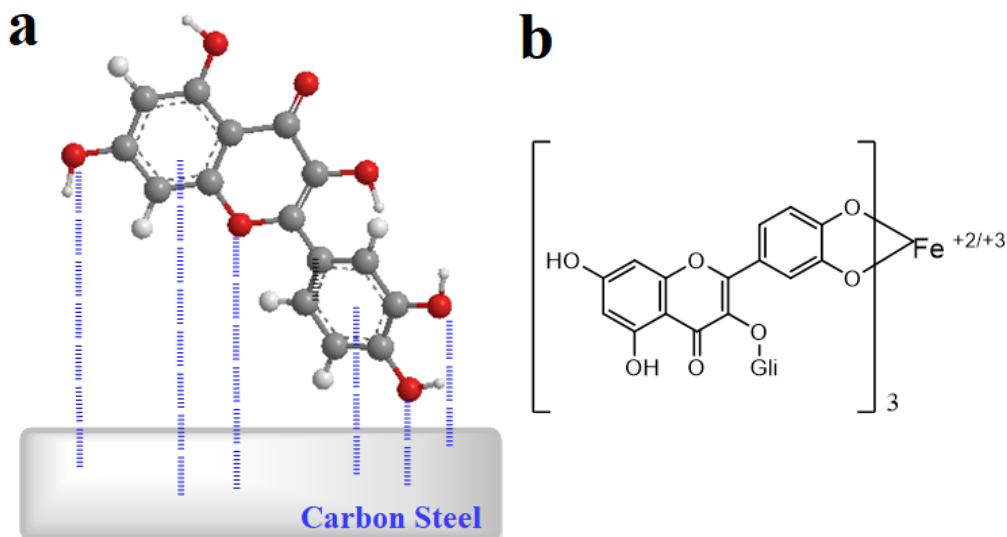


Figure 4. a) Flavonoid–metal surface interactions, b) Coordination complexes of quercetin glycoside - $\text{Fe}^{+2/+3}$.

3.3 Corrosion Tests

3.3.1 Mass loss

The mass loss tests on the A36 carbon steel were carried out over 24 hours at room temperature (25°C) in 0.1M NaCl and in the presence and absence of the apple peel extract at different concentration levels (100-1000 ppm). The results for inhibition efficiency percentage and corrosion rate are shown in Table 5 and Fig. 5. As expected, the corrosion rate falls with the increase in extract concentration, and therefore, the steel corrosion inhibition percentage by the extract increases, reaching a value of 88.77% at an extract concentration of 1000 ppm for the 24-hour test. This behaviour is due to adsorption of the organic compounds present in the extract, which block active sites on the metal.

Similar results were found by Ostovari et al. [31] for Henna extract, where the main components (Lawson, Gallic acid, α -D-Glucose and Tannic acid) are similar to those of Fuji apples. They obtained an inhibition of 88.89% at 1000 ppm of extract in 1M HCl solution.

Table 5. A36 carbon steel corrosion rate in 0.1M NaCl and inhibition percentage of the extract at different concentrations. Immersion time 24 hours at 25°C .

Carbon Steel/ 0.1 M NaCl solution + extract (ppm)	Corrosion rate (mm/year)	Inhibition (%)
Blank	0.901	-
100	0.427	52.60
250	0.335	62.82
500	0.222	77.33
1000	0.101	88.77

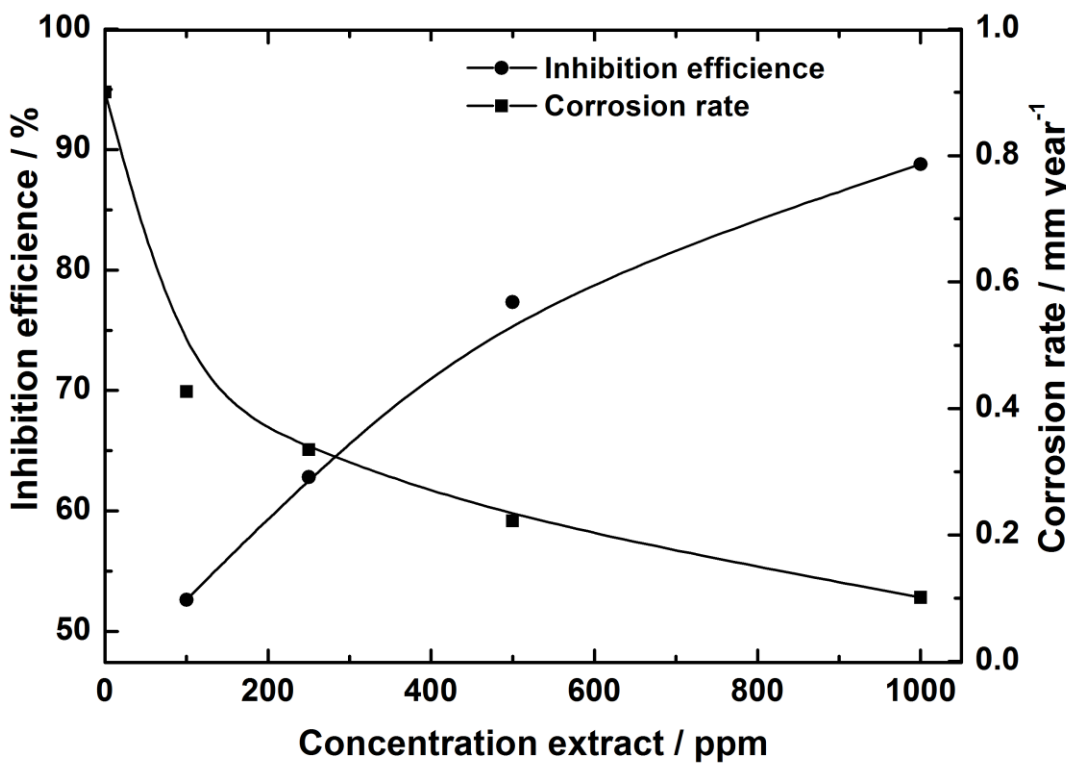


Figure 5. A36 carbon steel corrosion rate in 0.1M NaCl and inhibition efficiency of the extract. Immersion time 24 hours at 25°C.

Another mass loss experiment was carried out with 5 days of immersion in 0.1M NaCl in the presence and absence of the apple peel extract at a concentration of 1000 ppm, evaluating the variation over time of the open circuit corrosion potential. At the end of the experiment the potentials obtained were -526 mV vs SCE for the steel in the absence of the extract and -476 mV vs SCE in the presence of the extract, thus corroborating the inhibition effect of the extract with the increase in potential of 50 mV. This behaviour was observed by SEM (Fig. 6), where the steel in the absence of the extract (Fig. 6a) shows general corrosion with the formation of a porous corrosion product, identified as mainly Fe₂O₃. On the other hand, in Fig. 6b, in the presence of 1000 ppm of extract, no formation of corrosion product can be seen due to the adsorption of the organic compounds present in the extract. The EDS analysis shows the presence of mainly iron (Fe) and oxygen (O) on the steel surface, with an Fe/O ratio of 3.2 in the absence of the extract and 12.7 in the presence of the extract corroborating the increased formation of corrosion product in the absence of the extract.

In this corrosion assay the presence of the soluble iron ion in the solution was tested using UV spectrophotometry scanning at from 800 to 190 nm, aiming to evaluate the process of corrosion by general dissolution of the steel, obtaining iron salt as the product in solution.

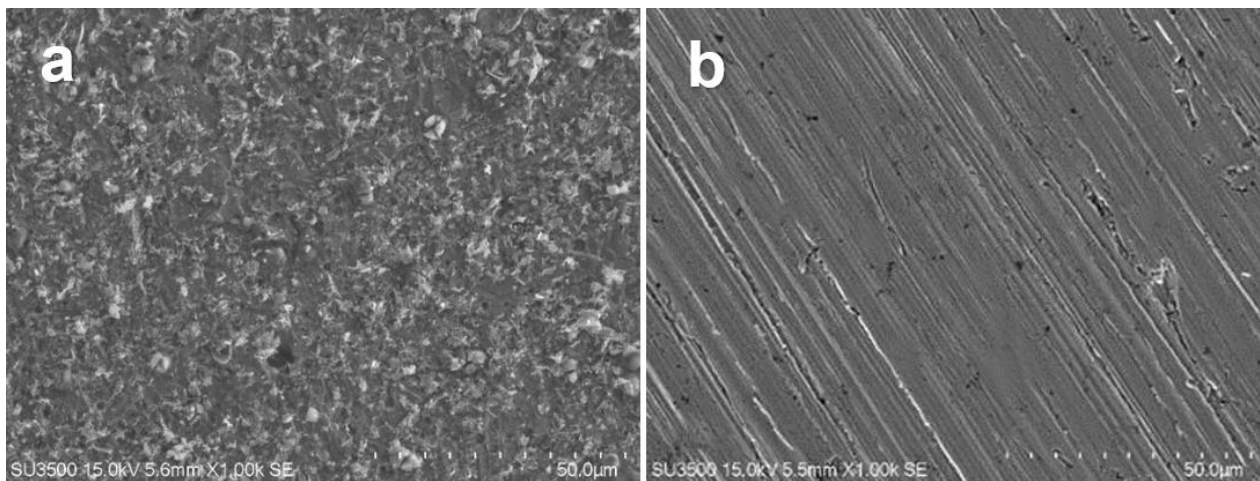


Figure 6. SEM of the A36 carbon steel after 5 days of immersion in 0.1M NaCl. a) Absence of the extract, b) Presence of the apple peel extract at 1000 ppm.

Fig. 7 shows the UV spectrum that confirms the presence of Fe^{2+} ions in the corrosion test without the extract, seen by the peak around 325 nm. In the same figure, no peak is seen when analysing only the extract solution and a very similar result is found for the test in the presence of 1000 ppm of extract, thus corroborating the inhibition of steel corrosion resulting from the Fuji apple peel extract. Comparing the two absorbencies obtained at 325 nm that indicate the presence of Fe^{2+} , the ratio obtained for A_0/A_e is 1.76, where A_0 is the absorbency measured in the solution without the extract after the test has run, and A_e is in the presence of the extract. The value of this ratio corroborates the inhibition of the steel corrosion as a result of the extract. Similar results were obtained by Karthiga et. al. [32] for beetroot extract with carbon steel in seawater.

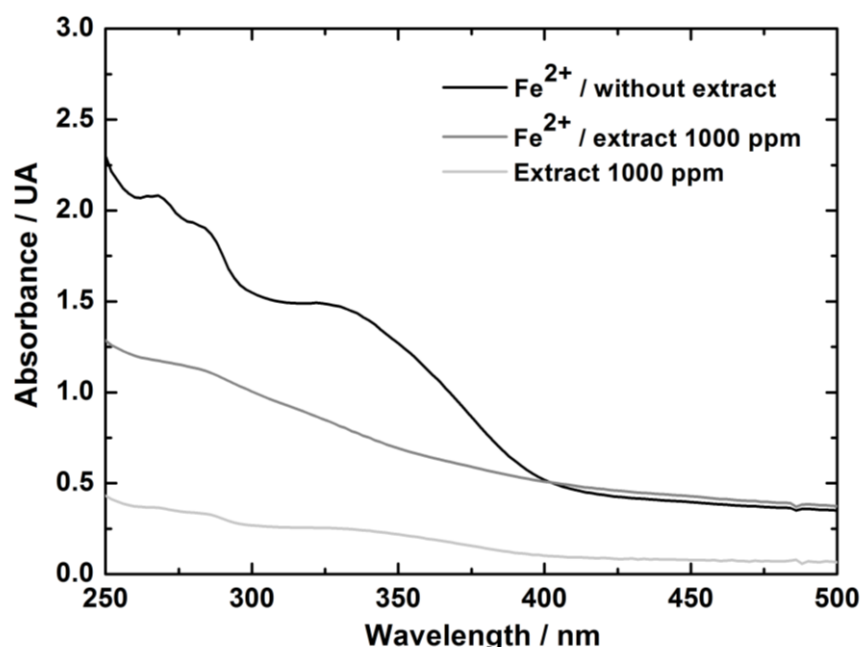


Figure 7. UV spectra of solutions obtained at the end of the mass loss test (5 days).

3.3.2 Electrochemical tests

3.3.2.1 Potentiodynamic polarisation curves

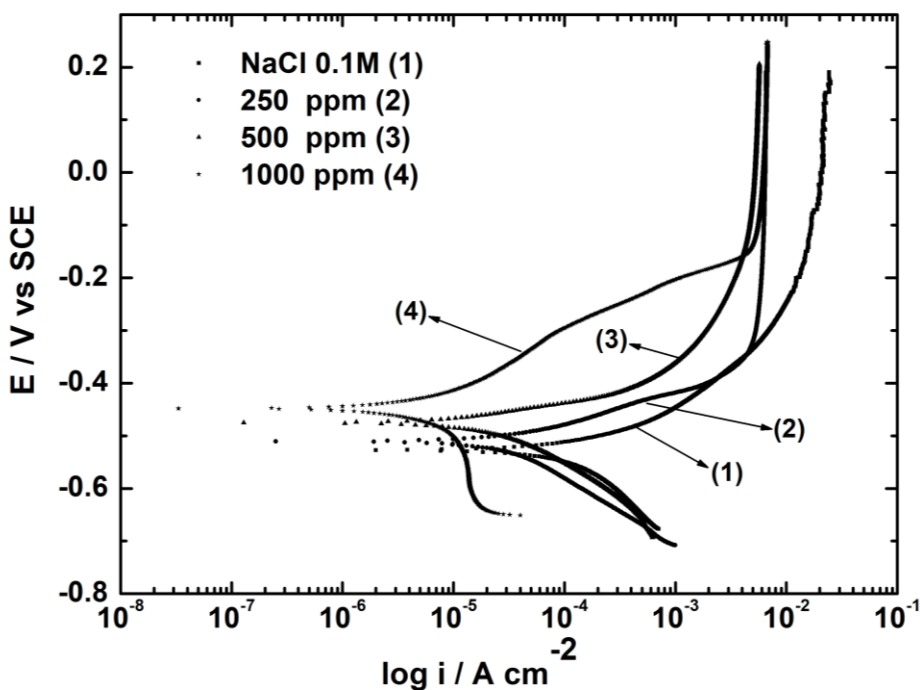


Figure 8. Tafel curves A36 steel in 0.1M NaCl at different extract concentrations at $25 \pm 1^\circ\text{C}$.

Fig. 8 shows Tafel potentiodynamic polarisation curves obtained in aerated conditions for the A36 carbon steel in 0.1M NaCl in the presence and absence of the apple peel extract at 25°C . The corrosion parameters obtained, including corrosion current density (I_{corr}), corrosion potential (E_{corr}), cathodic Tafel gradient (β_c), anodic Tafel gradient (β_a), and inhibition efficiency (η), are shown in Table 5.

Table 6 shows the displacement of the corrosion potential towards more positive values as the extract concentration increases, giving a shift of 80 mVsce comparing the steel without extract and in the presence of 1000 ppm of the extract. This potential displacement is similar to the results obtained for the open circuit described in part 3.3.1. The corrosion current falls (from 26.88 to $2.72 \mu\text{A}/\text{cm}^2$) with the increase in inhibitor concentration, and the inhibition percentage (η) reached at 1000 ppm of extract for the steel corrosion is 89.88%. Setting a potential of -300 mVsce, there is a clear difference in the current obtained for the anodic curve for the steel immersed in 0.1M NaCl in the absence and presence of 1000 ppm of extract, with values of $6.92 \times 10^{-3} \text{ A cm}^{-2}$ and $8.71 \times 10^{-5} \text{ A cm}^{-2}$, respectively.

This behaviour is due to the action of the polyphenolic organic components in the extract, which block active sites on the metal, decreasing anodic dissolution of the material and the cathodic reduction reaction of the oxygen (with an inhibitor concentration of 1000 ppm).

The Tafel gradients, both the anodic and cathodic, do not show significant variations when comparing the data in the absence and presence of the Fuji apple peel extract. This suggests that the

extract behaves as a mixed inhibitor, classified as adsorptive. This behaviour is similar to that obtained with Capsicum extract in the process of steel corrosion in 3.5% NaCl, which acts as a mixed inhibitor with efficiency of 92% [33].

Table 6. Tafel electrochemical parameters for A36 steel in 0.1M NaCl in the presence and absence of apple peel extract at 25°C.

Carbon Steel/ 0.1 M NaCl solution + extract (ppm)	Ecorr (mV SCE)	Icorr ($\mu\text{A cm}^{-2}$)	β_a (mV dec $^{-1}$)	β_c (mV dec $^{-1}$)	η (%)
Blank	-527	26.88	53.8	104.1	-
250	-515	11.23	63.5	84.1	58.22
500	-475	6.93	61.5	86.3	74.21
1000	-447	2.72	59.5	93.5	89.88

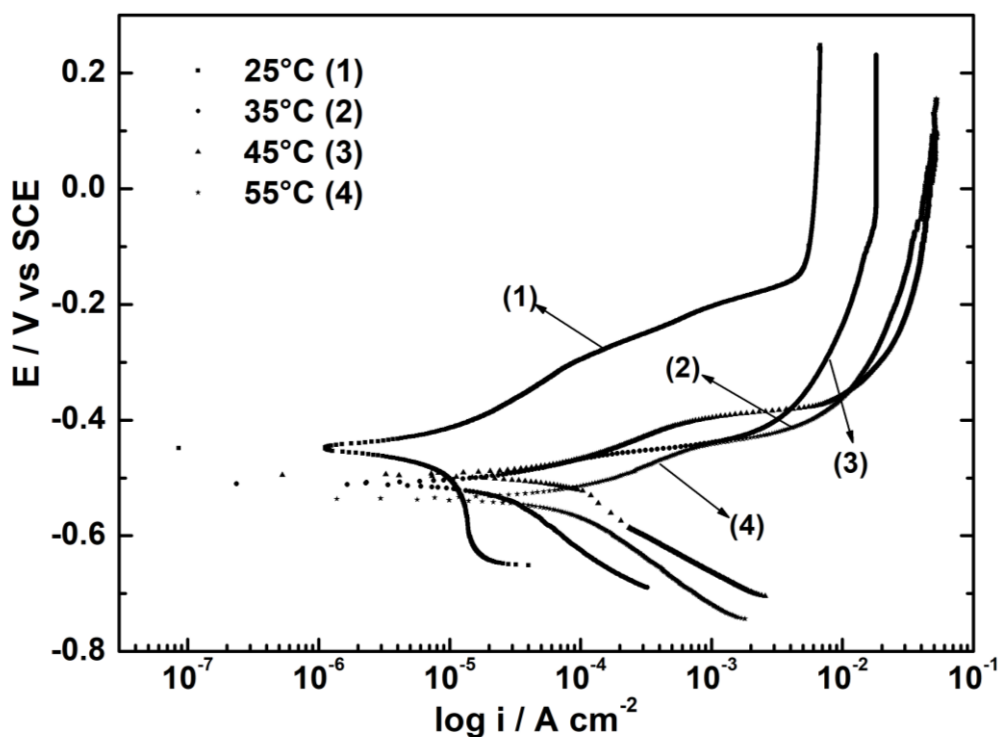


Figure 9. Tafel polarisation curves of apple peel extract (1000 ppm) at different temperatures.

Fig. 9 shows the Tafel polarisation curves for an extract concentration of 1000 ppm as a function of temperature (from 25°C to 55°C). It can be seen that as the temperature increases, there is a

rise in the corrosion current (from 2.72 to 36.05 $\mu\text{A cm}^{-2}$), indicating a decrease in the inhibitory effect on the steel corrosion of the Fuji apple peel extract. It can be noted that the anodic current is higher at 55°C, as seen in the active dissolution zone of the steel. The corresponding data are presented in Table 7.

Table 7. Electrochemical parameters as a function of temperature for the steel with and without the extract in 0.1M NaCl.

Temperature (°C)	Ecorr (mV vs SCE)	Icorr ($\mu\text{A cm}^{-2}$)	η (%)
25	-449.9	2.72	89.88
35	-510.2	12.8	80.64
45	-496.7	26.85	67.29
55	-535.4	36.05	61.65

3.3.2.2 Electrochemical Impedance Spectroscopy (EIS)

As in other studies of potentiodynamic curves, electrochemical impedance spectroscopy is a useful tool for analysis of the process of corrosion inhibition and the adsorption of organic molecules on the metal surface. Fig. 10 show Nyquist plots at different apple peel extract concentrations at 25°C, in which the resistance to charge transfer of the film formed on the steel surface (R_{ct}) and the electrical double layer capacitance (C_{dl}) can be seen. These are associated mainly with the dielectric nature of the film, whether it is a corrosion product or an inhibitor film.

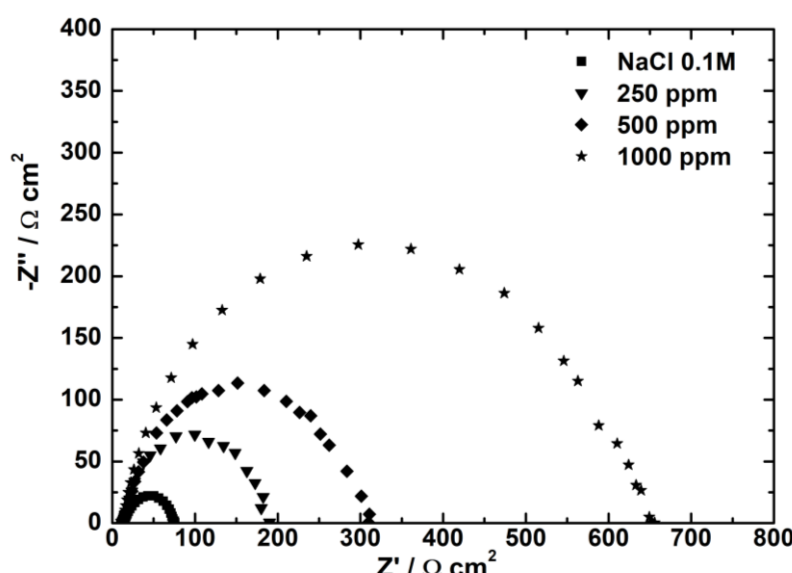


Figure 10. Nyquist plots at different apple peel extract concentrations for the steel in 0.1M NaCl.

The EIS data were filtered using the electric circuit shown in Fig. 11 and are presented in Table 8, where R_s and R_{ct} are the values for the solution resistance and the resistance to load transfer, respectively, and C_{dl} is the double layer capacitance. In order to take into account the effects of dispersion due to the roughness of the surface and other surface heterogeneities, C_{dl} is replaced by a constant phase element, CPE_{dl}, instead of an ideal double layer condenser [34]. CPE_{dl} is comprised of a Q_{dl} component, and an ' α ' coefficient that quantifies different physical phenomena, such as the non-homogenous surface due to roughness, inhibitor adsorption, the formation of porous layers, etc. [35]. The double layer capacitance was then calculated using the following formula:

$$C_{dl} = Q_{dl} (2\pi f_{max})^{\alpha-1} \quad (\text{equ. 5})$$

where, f_{max} is the frequency at the maximum height of the semicircle in the Nyquist plot.

The inhibitor efficiency percentage is calculated using the following equation:

$$IE (\%) = \left(\frac{R_{ct(inh)} - R_{ct}}{R_{ct(inh)}} \right) * 100 \quad (\text{equ. 6})$$

where, $R_{ct(inh)}$ and R_{ct} are the resistances to charge transfer in the presence and absence of the inhibitor, respectively.

The surface coverage of the organic molecules on the metal is represented by the symbol (θ) and is obtained from the following equation:

$$\theta = \frac{IE (\%)}{100} \quad (\text{equ. 7})$$

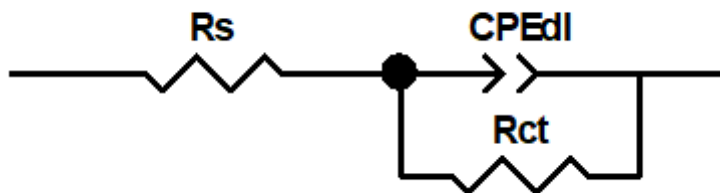


Figure 11. Equivalent circuit for the EIS data fitting.

Table 8. EIS data for the carbon steel in 0.1M NaCl in the presence and absence of different concentrations of apple peel extract.

Concentration (ppm)	R_s ($\Omega \text{ cm}^2$)	R_{ct} ($\Omega \text{ cm}^2$)	CPE _{dl} Q_{dl} (μMho)	CPE _{dl} α	C_{dl} ($\mu\text{F cm}^2$)	surface coverage (θ)	Inhibition IE (%)
Blank	12.82	63.02	655.61	0.74	188.28	-	-
250	13.83	177.38	343.35	0.66	84.01	0.64	64.47
500	13.21	296.78	196.68	0.72	64.87	0.79	78.77
1000	12.83	640.18	96.52	0.84	55.30	0.90	90.16

The Nyquist plots are symmetrical, forming the shape of a semicircle, thus indicating that the process of charge transfer takes place on the electrode/solution interface, with this process controlling the corrosion of the steel. As the extract concentration increases, the diameter of the semicircle also increases in the Nyquist plots, with a corresponding rise in the resistance to charge transfer from $63.02 \Omega \text{ cm}^2$ for the control (solution of 0.1M NaCl without the inhibitor) up to $640.18 \Omega \text{ cm}^2$, in the solution with the highest concentration of the inhibitor (1000 ppm). This is because the increase in extract concentration increases the adsorption of the constituent phytochemicals onto the metal surface, resulting in the formation of a protective layer that decreases electron transfer between the metal surface and the corrosive medium.

Furthermore, the decrease in C_{dl} values with the increased concentration, going from $188.28 \mu\text{F cm}^2$ (without the extract) to $55.30 \mu\text{F cm}^2$ (1000 ppm of extract) is attributed to the fall in the dielectric constant and/or the increase in the thickness of the electrical double layer, which in turn causes in increase in the volume of the layer of inhibitor, displacing the water molecules due to adsorption of the organic molecules from the extract and thus decreasing dissolution of the metal. The impedance test gave a corrosion inhibition percentage for the steel in 0.1M NaCl of 90.16% for the extract concentration of 1000 ppm. This value is in line with the result obtained for the mass loss (88.77%) and polarisation curves (89.88%).

The Bode plot and the phase angle show the capacitive behaviour of the steel. In the absence of the inhibitor the metal shows a rough non-homogenous surface due to the corrosion suffered in the saline medium, leading to a small angle and a low value for the impedance model. Both the Bode plot (Fig. 12a) and the phase angle (Fig. 12b) increase with the corresponding increase in extract concentration, reaching the highest phase angle (-65°) with the highest extract concentration level (1000 ppm), displacing the single peak to slightly lower frequencies due to the adsorption of organic molecules on the metal surface, reducing the surface irregularities.

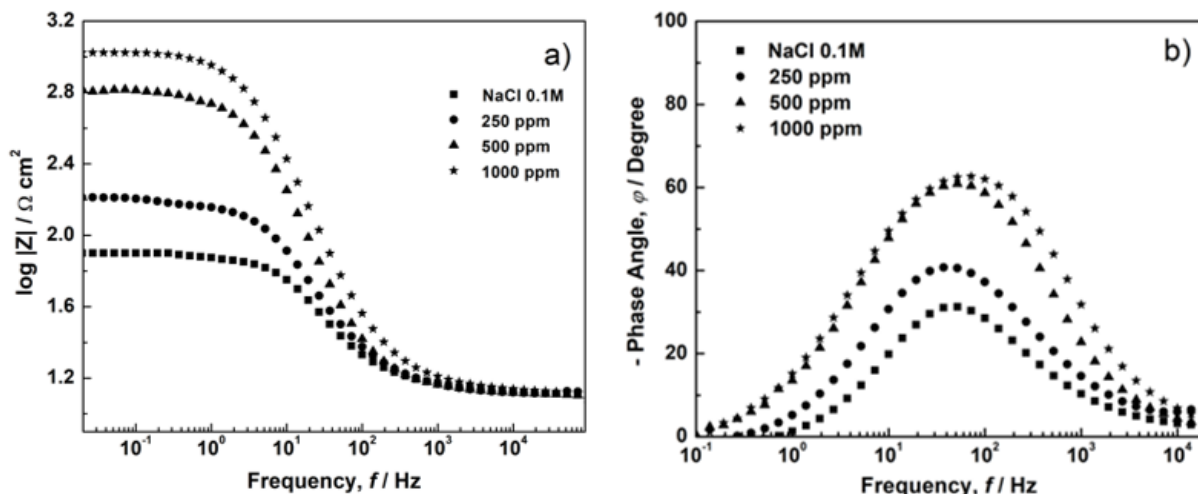


Figure 12. a) Bode modulus and b) Bode phase angle at different apple peel extract concentrations for the steel in 0.1M NaCl.

3.4 Adsorption Isotherm

Adsorption isotherms are generally used to elucidate on the inhibition mechanism of organic inhibitors on a metal surface. They provide information on the interactions of molecules adsorbed onto the metal surface and the interaction between the adsorbed molecules of the inhibitor. Surface coverage values were determined from the mass loss data for the 24-hour test at 25°C, assuming that the inhibition efficiency percentage (η) was directly proportional to surface coverage (Θ) [36].

In order to find the best fit for (Θ), some adsorption isotherms were considered, such as the Langmuir, Temkin, and Frumkin isotherms [37]. The surface coverage data were fit and the coefficient of correlation (R^2) was then used to select the best model of linearity, with the Langmuir isotherm found to provide the best description of the adsorption process on the metal. Fig. 13 shows the linear variation in $C/\theta / \text{g L}^{-1}$ as a function of the $C/\text{g L}^{-1}$ of the Cinh of the apple peel extract in 0.1M NaCl, thus corroborating that the adsorption is fit to the Langmuir adsorption isotherm, showing the adsorption of the adsorbate (the apple peel extract) onto the adsorbent (the steel). The data obtained from the graph is shown in Table 8.

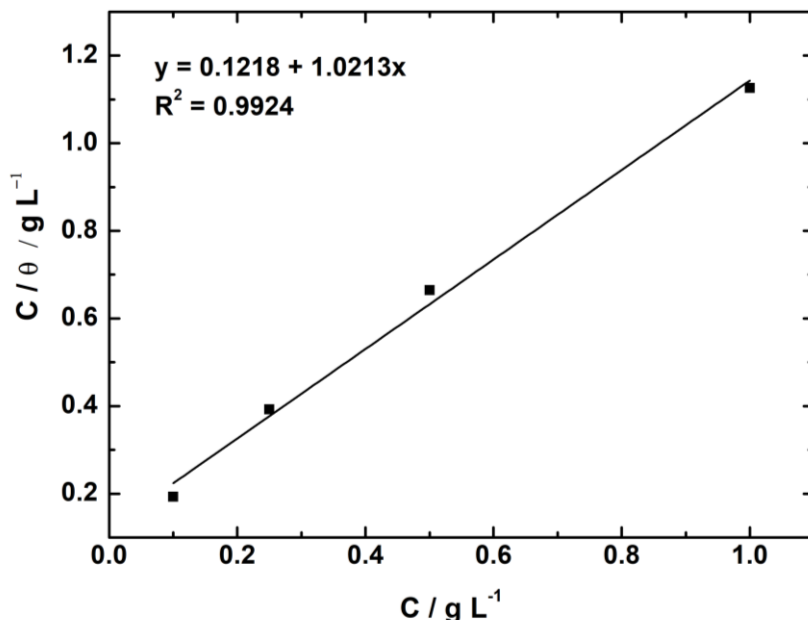


Figure 13. Langmuir isotherm for the adsorption of apple peel extract onto the surface of the carbon steel in the mass loss test in 0.1M NaCl.

The equilibrium constant (K_{ads}) for the adsorption process was estimated from the interception of the Langmuir isotherm and it was then used to calculate the Gibbs free energy of the adsorption ($\Delta G^{\circ\text{ads}}$) using equations 8 and 9:

$$\frac{C}{\theta} = \frac{1}{K_{\text{ads}}} + C \quad (\text{equ. 8})$$

$$K_{\text{ads}} = \frac{1}{55.5} \exp\left(\frac{\Delta G^{\circ\text{ads}}}{RT}\right) \quad (\text{equ. 9})$$

Table 9. Parameters of the Langmuir isotherm of the apple peel extract adsorbed onto the carbon steel surface.

Gradient	Intercept	Coefficient of correlation (R^2)	K_{ads}	ΔG^0_{ads} kJ/mol
1.021	0.122	0.995	8.21	-15.16

Table 9 also shows that the addition of apple peel extract leads to negative values for ΔG^0_{ads} , indicating that adsorption of the extract is a spontaneous process, similar to the results of Al-Senami et al. [38], who used cucumber peel to test steel in 1M HCl. Generally, values of ΔG^0_{ads} of up to -20 kJ/mol are consistent with the electrostatic interaction between charged inhibitor molecules and the carbon steel surface (physisorption) and values higher than -40 kJ/mol are interactions between the inhibitor molecules and the carbon steel surface to form a coordinated bond (chemisorption) [39-40]. For the apple peel extract, the value calculated (for ΔG^0_{ads}) was -15.16 KJ/mol, suggesting that the inhibition mechanism of the extract is physisorption.

4. CONCLUSIONS

Based on the experiment results, it has been shown that the Fuji apple peel extract from apples harvested in the central region of Chile can be used as a natural corrosion inhibitor for protection against corrosion of A36 steel in 0.1M NaCl.

The extract obtained from the apple peel contains 132.44 mm equivalent of Gallic Acid per gram of dry extract as phenolic content, while flavonoids present 99.15 mg equivalent of Quercetin per gram of dry extract. The main components are two flavones, one of which is a glycoside, while, at a lower proportion, there are two quercetin glycosides.

The Mass Loss corrosion test, Tafel Polarisaiton Curves and Electrochemical Impedance Spectroscopy (EIS) showed that as the concentration of the Fuji Apple Peel extract increases, so does the inhibition percentage, while the corrosion rate of the steel in the saline medium falls, reaching an inhibition percentage around 90%.

The adsorption process of the organic molecules in the apple peel extract respond to the Langmuir isotherm, corroborating the blocking of active sites on the steel sample. In the SEM analysis, it was seen that a smooth surface forms on the steel in the presence of the extract, compared to the rough surface seen with the absence of the extract. The value calculated for ΔG^0_{ads} was -15.16 KJ/mol, indicating that the inhibition mechanism of the apple peel extract is physisorption.

ACKNOWLEDGEMENTS

The authors gratefully acknowledge the Research Direction at the *Pontificia Universidad Católica de Valparaíso*, project number DI 037.460/2015.

References

1. D.D.N. Singh, T.B. Singh and B. Gaur, *Corros. Sci.*, 37 (1995) 1105.
2. A. Díaz-Gomez, R. Vera, A. Molinari, A. Oliva and W. Aperador, *Int. J. Electrochem. Sci.*, 10 (2015) 4004.
3. K.S. Parikh and K.J. Joshi, *Trans. SAEST*, 39 (2004) 31.
4. M. Faustin, A. Maciuk, P. Salvin, C. Roos and M. Lebrini, *Corros. Sci.*, 92 (2014) 287.
5. M.J. Bahrami and S.M.A. Hosseini, *Corros. Sci.*, 52 (2010) 2793.
6. D. Prabhu and P. Rao, *J. Env. Chem. Eng.*, 1 (2013) 676.
7. L.P. Tejeda Benítez, P.J. Castellar, P. Altamiranda and M.J. Berrocal Bravo, *Tech. Res.*, 78 (2014), 155.
8. R. Venegas, F. Figueredo, G. Carvallo, A. Molinari and R. Vera, *Int. J. Electrochem. Sci.*, 11 (2006) 3651.
9. W. Yang, Q. Wang, K. Xu, Y. Yin, H. Bao, X. Li, L. Niu and S. Chen, *Materials*, 10 (2007) 956.
10. T.H. Ibrahim, Y. Chehade and M. A. Zour, *Int J. Electrochem. Sci.*, 6 (2011) 6542.
11. M. Behpoura, S.M. Ghoreishia, M. Khayatkashania and N. Soltanib, *Mater. Chem. Phys.*, 131 (2012) 621.
12. A. Y. El-Etre, *Mater. Chem. Phys.*, 108 (2008) 278.
13. F. Bentis, M. Traisnel and M. Lagrenée, *Corros. Sci.*, 42 (2000) 127.
14. X. Li, S. Deng, H. Fu and T. Li, *Electrochim. Acta*, 54 (2009) 4089.
15. J. Yuri, A. Neira, F. Maldonado, A. Quilodrán, D. Simeone, I. Razmilic and I. Palomo, *J. App. Bot. Food Qual.*, 87 (2014) 131.
16. G. Giomaro, A. Karioti, A. Bilia, A. Buccini and L. Giampieri, *Chem Cent J.*, 8 (2014) 45.
17. I. Palomo, J.A. Yuri, R. Moore-Carrasco, A. Quilodrán and A. Neira, *Rev Chil Nutr.*, 37 (2010) 377.
18. A. Francini and L. Sebastiani, *Antioxidants*, 2 (2013) 181.
19. A. Silveira, C. Sautter, S. Tonetto de Freitas, G. Galieta and A. Brackmann, *Ciênc. Tecnol. Aliment.*, 27 (2007) 149.
20. Z. Mengxia, Z. Guojing, Y. Yaohua, Y. Chengquan, L. Pengmin and M. Fengwang, *Sci Horticult.*, 201 (2016) 18.
21. V. L. Singleton, R. Orthofer and R.M. Lamuela-Raventós, *Meth in Enz.*, 299 (1999) 152.
22. M. J. Simirgiotis, M. Silva, J. Becerra and G. Schmeda-Hirschmann, *Food Chem.*, 131 (2012) 318.
23. ASTM G31-72 (2004). Standard practice for Laboratory Immersion Corrosion Testing of Materials. *ASTM International*, West Conshohocken, PA, 2004. www.astm.org.
24. ASTM G1-03 (2002). Standard practice for Preparing, Cleaning and Evaluating Corrosion Test Specimens. *ASTM International*, West Conshohocken, PA, 2002. www.astm.org.
25. N.A. Odewunmi, S.A. Umoren and Z. M. Gasem, *J. E. Chem Eng.*, 3 (2015) 286.
26. V. Vasconcelos Torres, R. Salgado Amado, C Faia de Sá, T. C. López Fernandez, A. da Silva Riehl, A. Guedes Torres and E D'Elia, *Corros. Sci.*, 53 (2011) 2385.
27. M. Hunsom, P. Saila, P. Chaiyakam and W. Kositnan, *Int. J. Ren Ener Res.*, 3 (2013) 362.
28. H. Zhu, Y. Wang, Y. Xia and T. Tang, *Food Anal. Methods.*, 3 (2010) 90.
29. V. Quitral, M. Sepúlveda and M. Schwartz, *Rev. Iber. Tecnología Postcosecha.*, 1 (2013) 3.
30. A. Schieber, P. Keller and R. Carle, *J. Chromatograph A.*, 910 (2001) 265.
31. A. Ostovari, S. M. Hoseinieh, M. Peikari, S. R. Shadizadeh and S. J. Hashemi, *Corros. Sci.*, 51 (2009) 1935.
32. N. Karthiga, S. Rajendran, P. Shantha, A. Krishnaveni and J. Jeyasundari, *Int. J. Nan. Corros. Sci. Eng.*, 5 (2015) 255.
33. C. G. Vaszilcsin, M. L. Dan, A. F. Enache and I. Hulka, *Chem Bull.*, 75 (2016) 23.
34. I.D. Raistrick, J.R. MacDonald and D.R. Franceschetti, John Wiley & Sons, New York, (1987).
35. X. Li, S. Deng and H. Fu, *Corros. Sci.*, 3 (2009) 485.

36. Z. Wang, Y. Gong, C. Jing, H. Huang, H. Li, S. Zhang and F. Gao, *Corros. Sci.*, 113 (2016) 64.
37. W. Li, Q. He, C. Pei and B. Hou, *Electrochim. Acta*, 52 (2007) 6386.
38. M. Al-Senani, *Int. J. Electrochem. Sci.*, 11 (2016) 291.
39. H. Tian, W. Li, K. Cao and B. Hou, *Corros. Sci.*, 73 (2013) 281.
40. E. Stupnisek-Lisac, A. Gazivoda and M. Madzarac, *Electrochim. Acta*, 47 (2002) 4189.

© 2018 The Authors. Published by ESG (www.electrochemsci.org). This article is an open access article distributed under the terms and conditions of the Creative Commons Attribution license (<http://creativecommons.org/licenses/by/4.0/>).